

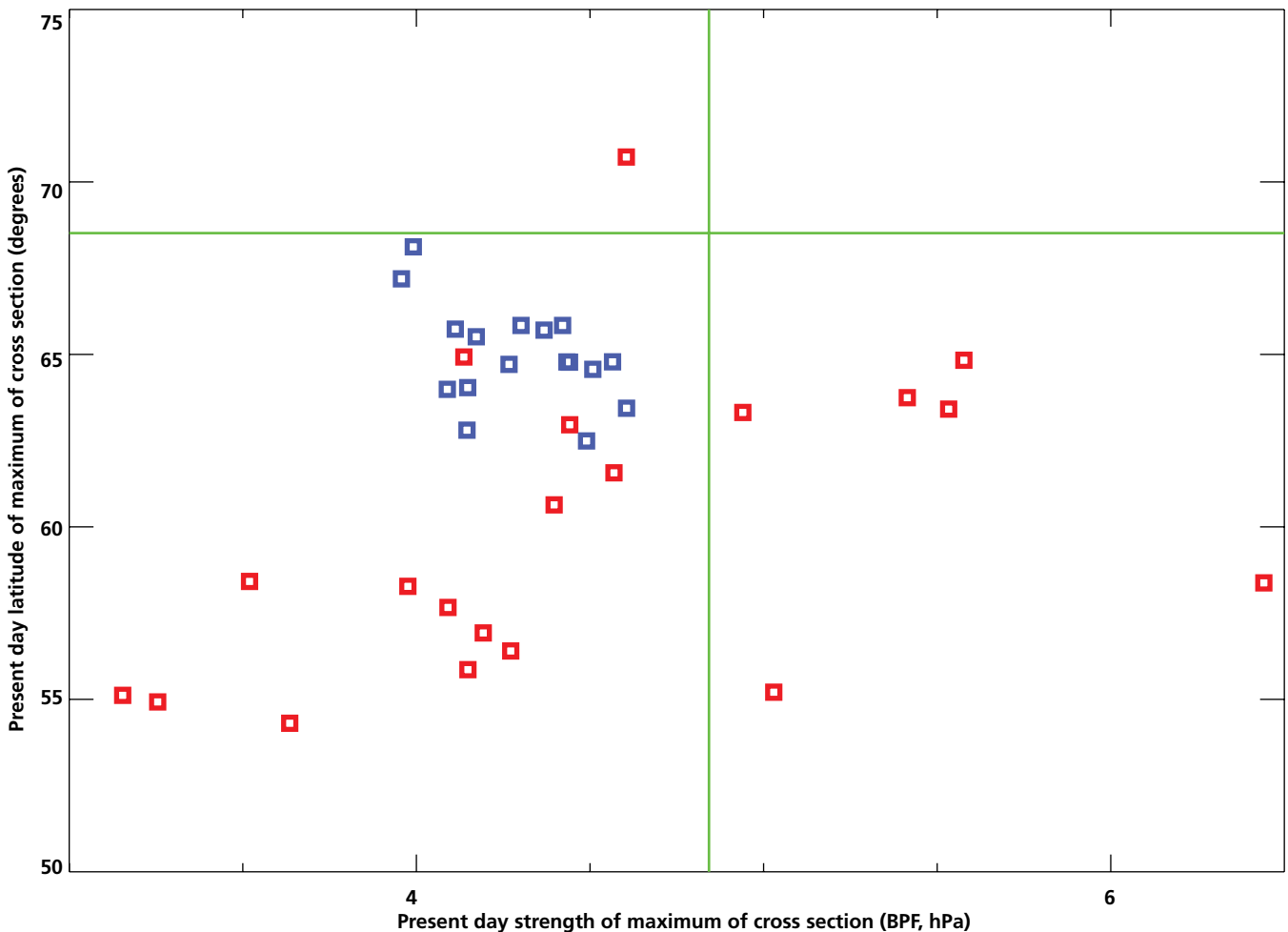
some having strengths as much as 20% too low. However, this spread is smaller than that seen in the CMIP3 multi-model ensemble, where the equivalent range is from 2 degrees too far north to 14 degrees too far south, and range in intensity from 35% too low to 33% too high (Figure A3.6).

Feature-tracking software has also been used to investigation of storms and storm-tracks in these rather coarse-resolution climate models (see Annex 6). Experience tells us, however, that much higher resolution numerical models, such as those used for weather prediction with grid-lengths of the order of 10s of kilometres rather than 100s of kilometres, show much greater fidelity in their ability to simulate the details of individual storms, fronts, etc. that are familiar from looking at daily weather maps. Tropical cyclones which may re-curve into mid-latitudes and become intense storms cannot, for example, be simulated by the current generation of climate models. That is not to say however that such storms are likely to form a major component of the climate change signal. At present, such storms are relatively rare (although may have large consequences) and there is no robust evidence that their frequency will change in the future. Nevertheless, without a number of relatively high-resolution climate model simulations, which will take many years if not decades to realise, it is almost impossible to make any reliable assessments of such phenomena.

**(b) Anticyclones and blocking**

NW Europe, and in particular the UK, are preferred regions of the globe for anticyclonic events by virtue of being at the end of the Atlantic storm track. The examination of anticyclones turns out to be more complex than the case of

**Figure A3.6: Present-day location and intensity of the North Atlantic storm track at the longitude of the UK. The blue squares are from the 17-member HadCM3 perturbed physics ensemble (PPE\_A1B in Chapter 3) and the red squares are from the CMIP3 multi-model ensemble. The green lines are from ERA40, and can be thought of as the observed position and strength.**



cyclone activity and three different measures have been used to evaluate the ensemble. The inconsistency of the three diagnostics makes it difficult to make a clear statement about the ability of the perturbed physics ensemble to simulate anticyclones, but in general the HadCM3 ensemble is competitive with other climate models.

Further information may be gleaned from the analysis of a particular anticyclonic phenomenon, that of atmospheric blocking. Blocking situations, whereby areas of relatively immobile high atmospheric pressure tend to dominate weather patterns for many days, result in relatively cold, still conditions often accompanied by fog in winter. In summer they tend to be accompanied by dry sunny conditions and heatwaves.

The mechanisms for atmospheric blocking are only partially understood, but it is clear that there are complex motions, involving meso-scale atmospheric turbulence, and interactions that climate-resolution models may not be able to

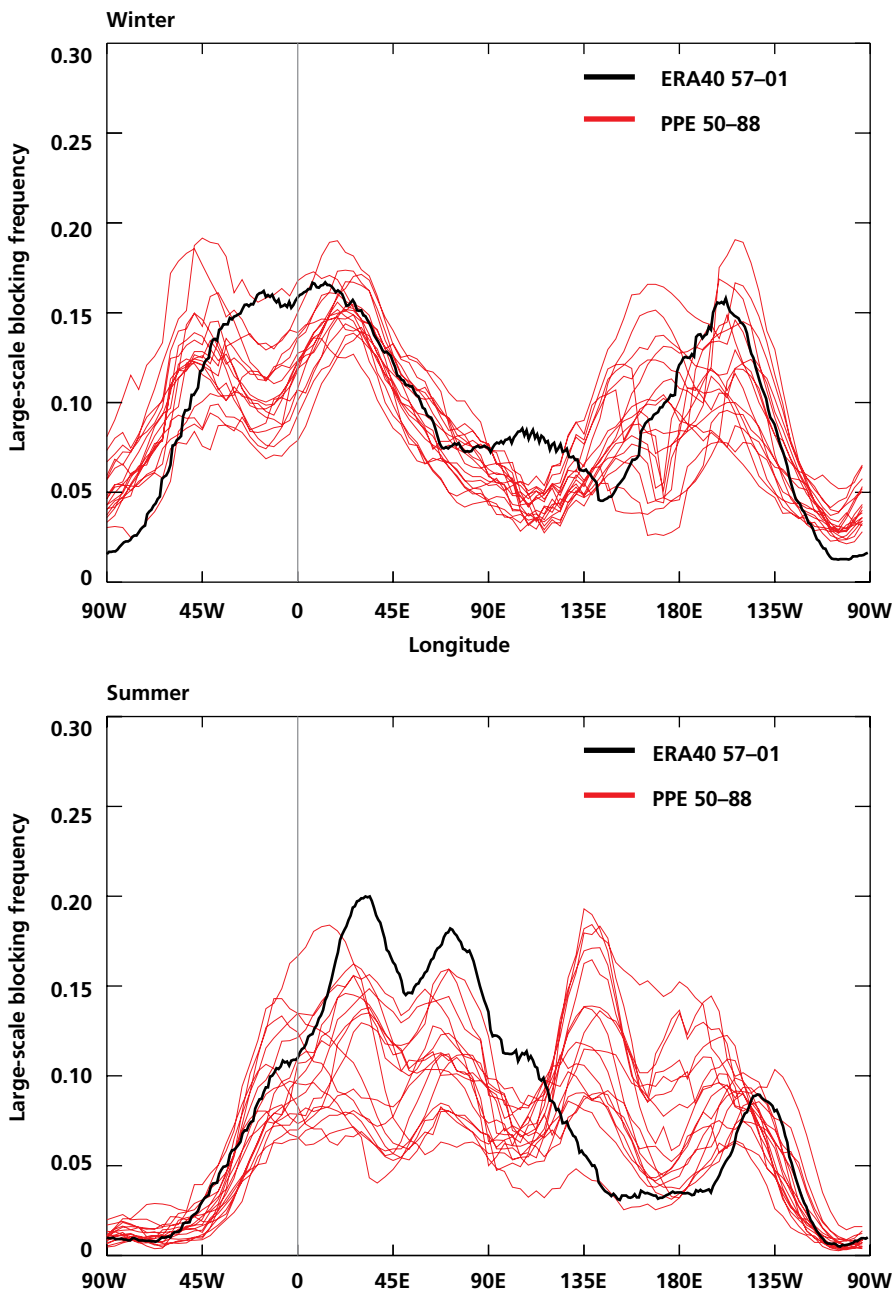
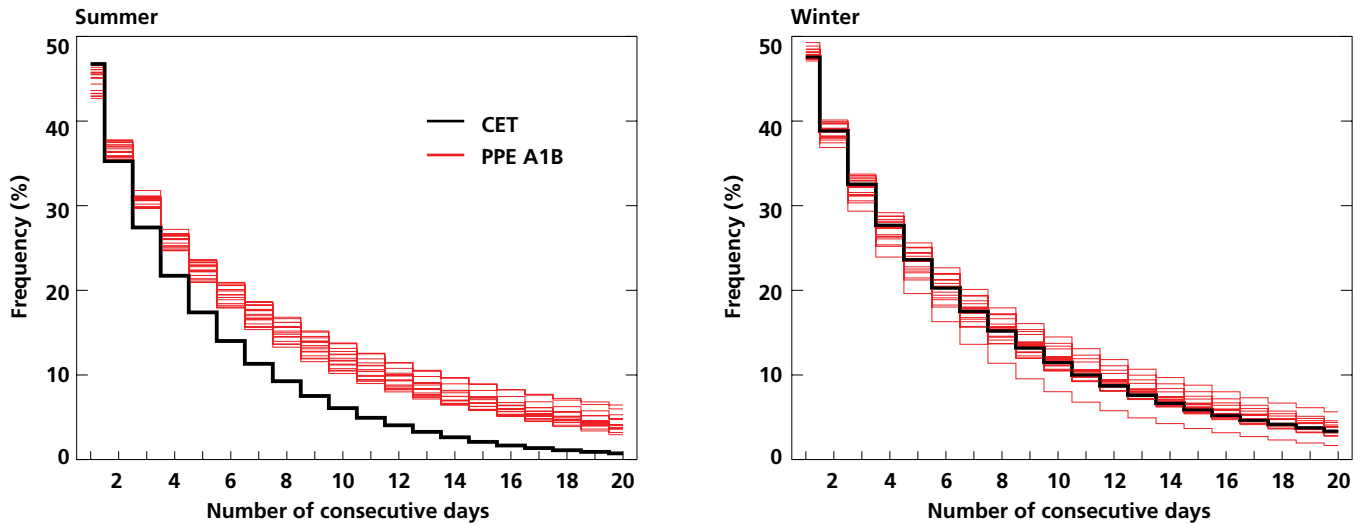


Figure A3.7: The frequency of blocking events in the perturbed physics HadCM3 ensemble (PPE\_A1B, red lines) for winter (DJF, top) and summer (JJA, bottom) together with that estimated from ERA40 (thick black lines). The blocking index is calculated following Pelly and Hoskins (2003) and uses a variable latitude to track the location of the model storm track (in contrast to other indices which used a fixed latitude).



represent fully. The prediction of the intensity and duration of blocking events is one of the most difficult weather forecasting situations. The HadCM3 model does represent, with reasonable fidelity, some aspects of present-day atmospheric blocking in the North Atlantic region (see Figure A3.7) with the performance in summer better than that in winter. At other longitudes the model shows less fidelity, in particular in the Pacific sector. (An additional complication is that it is not clear that simply doubling the resolution of a climate model automatically produces a better simulation of blocking — in the case of one Met Office Hadley Centre model, this results in a degradation).

The role of atmospheric blocking under climate change is currently a major topic of research. Might current model errors severely limit the reliability of climate change projections (e.g. Palmer *et al.* 2008; Scaife *et al.* 2008)? Might large changes in blocking, that current models cannot simulate, cause large changes in the frequency of occurrence of summer heat waves for example? Of more practical interest than the diagnosis of blocking frequency is perhaps is the frequency of occurrence of blocking-like weather in the models used in UKCP09. Figure A3.8 shows a diagnostic of occurrences of periods of cold winter and warm summer days in the UK in the PPE\_A1B ensemble. For the winter case, each model in the ensemble does a reasonable job of simulating the relative frequency of occurrence of cold spells. In the summer, the model versions overestimate the frequency of occurrence of warm spells (despite the blocking frequency diagnostic being close to that observed around the Greenwich Meridian in Figure A3.7 — other processes are important). Careful evaluation of such diagnostics from the RCM simulations and the weather generators is recommended in cases where such variability is important to the individual user. It should be noted that the UKCP09 PDFs of mean changes and extremes include, by definition, the effects of blocking and changes in blocking from both perturbed physics and multi-model ensembles. Changes in the storm-tracks and blocking are presented in Annex 6.

### A3.5 The effect of mean biases in models

**The probabilistic approach quantifies uncertainties in the processes and feedbacks associated with summer drying and related impacts.**

As highlighted above, biases in present-day summer climates in models are an issue and may effect the response of the model under climate change. Rowell and Jones (2006) examined the different mechanisms for future summer drying

**Figure A3.8: The frequency of occurrence of consecutive days of same-sign temperature anomalies from the Central England Temperature (CET) record (black line) and from an equivalent diagnostic from the 17-member ensemble of perturbed physics HadCM3 (PPE\_A1B – red lines). On the left panel there is, by definition, a near 50% chance of a day being warmer than average, a 35% of getting two consecutive warm days, etc. On the right panel, the chance of getting consecutive cold days in winter is plotted.**

and Jones (2006) examined the different mechanisms for future summer drying under climate change using a matrix of global and regional model experiments. They found that the primary drivers for summer drying in continental Europe are the direct warming coming from enhanced greenhouse gases, coupled with a tendency for a more rapid decline in spring soil moisture which pre-conditions the soil to be dryer prior to the onset of summer. If the soil is moist, then some of the solar heating will be channelled into evaporating this moisture. If the soil is drier, then more of the solar heating will be available to increase temperatures. They also found that the summer soil moisture feedback, whereby reduced soil moisture leads to an increase in surface sensible heating which further reduces soil moisture, was important. Hence future changes in regional climate are driven by a complex array of processes, dependent on both local and remote factors which are included in climate models. Systematic local and remote errors might impact the response derived only from HadCM3 ensembles, but by including results from other models through the discrepancy terms ameliorates this possibility.

In the model experiments used to produce the PDFs presented in this report, a number of processes which control these various feedbacks are perturbed (for example, the number of soil levels accessed for evapotranspiration). Thus we have attempted to explore the uncertainties in the mechanisms for summer drying by using model output from perturbed physics and from multi-model ensembles.

### A3.6 Discussion

This annex gives a flavour of some of the issues in climate modelling, with some focus on physical processes that have been major topics of discussion in recent times. A key point is that the UKCP09 PDFs are designed to sample much of the uncertainty introduced by deficiencies in climate models by the use of perturbed physics and multi-model ensembles which in the case of PPEs are weighted by their ability to simulate historical mean climate and climate change. The PDFs represent a measure of the credibility of our current ability to predict climate change.

Much work in climate change research is directed towards both improving climate models and understanding how model deficiencies might impact the magnitude and spatio-temporal pattern of climate change. This research will eventually feed-through to more credible predictions, i.e. PDFs with less uncertainty. Nevertheless, there is a possibility that changes and improvements to models might reveal extreme or very different patterns of climate change outside the range of the UKCP09 PDFs. While we have endeavoured to capture the major feedbacks and their uncertainties and to account for the major deficiencies in models, only future research will be able to tell us if this is the case.

### A3.7 References

- Gillett, N. P. (2005). Northern Hemisphere circulation, *Nature*, **437**, 496.
- Greeves, C. Z., Pope, V. D., Stratton, R. A. & Martin, G. M. (2007). Representation of northern hemisphere winter storm tracks in climate models. *Climate Dynamics*, **28**, 683–702.
- Hoerling, M. P., Hurrell, J. W. & Xu, T. (2001). Tropical origins for recent North Atlantic climate change. *Science*, **292**, 5514, 90–92.
- Palmer, T. N., Doblas-Reyes, F. J., Weisheimer, A. & Rodwell, M. J. (2008). Toward seamless prediction: calibration of climate change projections using seasonal forecasts. *Bulletin of the American Meteorological Society*, 459–470.
- Pelly, J. L. & Hoskins, B. J. (2003). A new perspective on blocking. *Journal of Atmospheric Science*, **60**, 643–755.
- Rodwell, M. J., Rowell, D. P. & Folland, C. (1999). Ocean forcing of the wintertime North Atlantic Oscillation and European climate. *Nature*, **398**, 320–323.
- Rowell, D. P. & Jones, R. G. (2006). Causes and uncertainty of future summer drying over Europe. *Climate Dynamics*, **27**, 281–299.
- Scaife, A. A., Knight, J. R., Vallis, G. K. & Folland, C. K. (2005). A stratospheric influence on the winter NAO and North Atlantic surface climate. *Geophysical Research Letters*, **32**, L18715.
- Scaife, A. A., Buontempo, C., Ringer, M., Sanderson, M., Gordon, C. K. & Mitchell, J. (2009). Comment on *Toward seamless prediction: calibration of climate change projections using seasonal forecasts*. *Bulletin of the American Meteorological Society*, Accepted.
- Solomon, S. et al. (2007). *IPCC Climate Change 2007: The Physical Science Basis. Contribution of Working Group 1 to the Fourth Assessment Report of the Intergovernmental Panel on Climate Change*. Cambridge University Press.
- Stephenson, D. B., Pavan, V., Collins, M., Junge, M. M. & Quadrelli, R. (2006). North Atlantic Oscillation response to transient greenhouse gas forcing and the impact on European winter climate: A CMIP2 multi-model assessment. *Climate Dynamics*, **27**(4), 401–420.
- Stott, P. A., Tett, S. F. B., Jones, G. S., Allen, M. R., Mitchell, J. F. B. & Jenkins, G. J. (2000). External control of twentieth century temperature by natural and anthropogenic causes. *Science*, **290**, 2133–2137.
- Sutton, R. & Hodson, D. (2007). Climate response to basin-scale warming and cooling of the North Atlantic Ocean. *Journal of Climate*, **20**(5) 891–907.

## Annex 4: Probabilistic projection data

The maps and graphs shown in this report, and others available from the UKCP09 website, are generated from a large dataset of probabilistic projections. Chapter 3 describes the methodology developed to produce the projections, and in particular Section 3.2.11 describes the various stages of the procedure. Out of this emerge two products which are described in this annex.

*Ag Stephens, British Atmospheric Data Centre*

### A4.1 Cumulative distribution functions

The first product from the User Interface is a series of cumulative distribution functions (CDFs). Each of these consist of a set of 107 values of future climate changes corresponding to a set of 107 pre-defined probability levels. These CDFs are provided for each variable at each location, temporal average, future time period and emissions scenario. This is the data which is used to form the CDF or PDF graphs (and plume plots) available from the User Interface, such as those shown in Chapter 4. The set of CDFs for every 25 km square in the UK is used to form maps at the 10, 50 and 90% probability levels, such as those also shown in Chapter 4.

Different probability levels have different levels of robustness. We believe data for probability levels between 10 and 90% to be robust. Probability levels between 1 and 9% and 91 and 99% are to be used with caution as these are less robust and the level of robustness will vary according to which variable is being used. Probability levels less than 1% and greater than 99% are only included so that users can generate plots of PDFs estimated from this CDF data to a similar standard found in the UKCP09 User Interface.

### A4.2 Sampled data

Users require values sampled from CDFs to input into their impacts models. For one variable of interest this could be sampled from the appropriate CDF. But most impact models will require more than one variable and it is important to capture in the sampling procedure how these variables depend on each other. The second product described in this annex, referred to as *sampled data* satisfies this requirement and can be thought of as a spreadsheet (Table A4.1); there

are actually two\* spreadsheets (known as Batch 1 and Batch 2) for each 25 km grid square and aggregated region (per emissions scenario and per future time period). Each spreadsheet has 10,000 samples (rows), which have been sampled according to weight (a relative measure of how well an individual model variant compares to observations) from a much larger number generated by the probabilistic statistical methodology (see Chapter 3, Section 3.2.11). Each row can be thought of as representing projections at a single location from a single model variant; so the sampled data can be used to look at a consistent set of changes in the seasonal cycle of a climate variable but not at a consistent set of changes at different locations. As the sampling was done by weight, each row can be considered as equi-probable; sampling allows the better model variants to be selected several times within the sampled data set, and rows from the same model variant have the same mean climate change but differ in how the noise was sampled. The columns of each spreadsheet consist of a number of variables for each temporal averaging period. Figure A4.1 shows schematically the variables, emissions scenarios, locations, time periods and temporal averages.

Smaller numbers of rows can be sub-sampled randomly, but the smaller the sub-sample, the greater the chance of the distribution diverging from that of the full sampled population of 10,000. Also, rows can be specified by sample i.d. but this approach requires careful consideration and justification and could lead to a biased decision if used incorrectly. Similar spreadsheets are available for some variables as future climate, rather than climate change, in which the changes have been combined with an observed 1961–1990 climatology. Data sampled from this spreadsheet (for example, changes in precipitation and temperature for a particular 25 km square) can be used as input to an impacts model.

Note that the sampled data has been clipped using the 1 and 99% probability levels from the CDF data for all available variables. That is, for a given combination of variable, location, time period, averaging period and emission scenario, the values of sampled data below the 1% probability level are set to the value of the 1% probability level from the corresponding CDF, and values above the 99% probability level are set to the value of the 99% probability level.

The User Interface will allow downloading the sampled data directly; as this is about 0.5 Tbytes in all, users are guided towards defining a suitable subset for their needs. The user could download the data from this request as a csv or CF-netCDF file; the csv option would allow the data to be imported into, and manipulated using, a standard desktop spreadsheet package.

A typical request might be:

- **Variables?** *Mean temperature, mean precipitation*
- **Climate change or future climate?** *Climate change*
- **Emissions scenario?** *High*
- **Location?** *25 km grid box 1628 (London)*
- **Time period?** *2070–2099*
- **Temporal average?** *Winter and Summer*
- **Number of subsamples?** *Random selection of 1000 (of the 10,000 possible samples)*

---

\* Due to limitations in processing, all the variables cannot be included in a single spreadsheet and each location is processed separately.

Low emissions, Grid box 1234, Batch 1						Low emissions, Grid box 1234, Batch 2			
2020s						2020s			
January					Feb...Dec	January			Feb...Dec
Sample i.d.	Tmean	Tmax	Tmax99%	Tmin...	Tmean, Tmax...	Sample i.d.	MSLP	RH...	MSLP, RH...
0	3.3	4.4	5.5			0			
1	3.8	4.8	5.8			1			
...						...			
9999	2.9	4.1	5.1			9999			

Table A4.1: Diagrammatic representation of a segment of the two batches of data for one 25 km grid square under one emissions scenario and for one future time period.

VARIABLE (17)	EMISSIONS SCENARIO (3)	SPATIAL AVERAGE:	TIME PERIOD (7)	TEMPORAL AVERAGE (17)	SAMPLE NUMBER (10,000)
Mean daily temperature Mean daily maximum temperature Mean daily minimum temperature 99th percentile of daily maximum temperature 1st percentile of daily maximum temperature 99th percentile of daily minimum temperature 1st percentile of daily minimum temperature Precipitation rate 99th percentile of daily precipitation rate Specific humidity Relative humidity Total cloud Net surface long wave flux Net surface short wave flux Total downward shortwave flux Mean sea level pressure  (some variables can be provided as both climate change and future climate)	Low (B1) Medium (A1B) High (A1FI)	25 km Grid box (440 land cells) <i>or</i> Administrative region (16) <i>or</i> River basin (23) <i>or</i> Marine region (9)	2010-2039 (2020s) 2020-2049 (2030s) 2030-2059 (2040s) 2040-2069 (2050s) 2050-2079 (2060s) 2060-2089 (2070s) 2070-2099 (2080s)	Jan Feb Mar Apr May Jun Jul Aug Sep Oct Nov Dec Winter (DJF) Spring (MAM) Summer (JJA) Autumn (SON) Annual  (Not all variables are available at monthly resolution)	0 1 2 ... ... 9,998 9,999

Figure A4.1. Structure of the UKCIP09 Probabilistic Sampled Data for one batch. Some variables can be provided as both climate change and future climate. Not all variables are available at monthly resolution.

Batch 1	Batch 2
Mean temperature*	Specific humidity
Mean daily maximum temperature	Net surface long wave flux
Mean daily minimum temperature	Net surface short wave flux
99th percentile of daily maximum temperature	Total downward shortwave flux
1st percentile of daily maximum temperature	Mean sea-level pressure
99th percentile of daily minimum temperature	Lag-1 correlation of daily precipitation* #
1st percentile of daily minimum temperature	
Precipitation rate (percentage change)*	
99%ile of daily precipitation	
Relative humidity*	
Total cloud	
Variance of daily precipitation* #	
Skewness of daily precipitation* #	
Probability of a dry day* #	
Variance of daily mean temperature* #	

**Table A4.2: Allocation of variables between the two batches; joint probabilities can be calculated between variables in the same batch only.**  
 \* These variables are required to condition the Weather Generator (UK Climate Projections Science report: Projections of future daily climate for the UK from the Weather Generator). # These variables are not available from the User Interface.

Changes (a) with different emissions scenarios, (b) at different locations and (c) in different batches, are not coherent and therefore cannot be combined. If users require a joint probability of changes in two variables, then plots can be provided directly by the User Interface (see Chapter 4, Section 4.6). If users require the joint probability of changes in more than two variables, they can download the variables and perform the necessary calculations offline using their own statistical packages. Joint probabilities (see example in Chapter 4, Section 4.6) can only be created for groups of variables in the same batch; the variables in each batch have been selected to cater for the combinations of variables needed to run the Weather Generator; see Table A4.2 (overleaf). Examining joint probabilities between variables in different batches is inadvisable, and hence the User Interface will not enable this.

## Annex 5: Changes to the Atlantic Ocean circulation (Gulf Stream)

### A5.1 How does the Atlantic Ocean circulation influence UK climate?

The climate of the UK is influenced by its proximity to the North Atlantic Ocean. The ocean acts as a buffer, absorbing heat in the summer and releasing it in the winter, and so moderating the seasonal cycle of temperature. The ocean also supplies moisture to the atmosphere, some of which falls as precipitation over the UK. These climatic influences are expected to continue under plausible scenarios of climate change.

A further influence of the ocean, which is susceptible to change in future, comes from the *Meridional Overturning Circulation* in the North Atlantic (MOC, sometimes less precisely referred to as *thermohaline circulation*, *conveyor belt circulation* or *Gulf Stream circulation*). Surface circulation in the North Atlantic brings warm and relatively salty water northwards from the subtropics. During transit northward, some of the heat is lost to the atmosphere, particularly in the Northwest Atlantic and Nordic Seas. The resulting cold, salty (and hence dense) water sinks and returns southwards several kilometres below the surface. The MOC thus supplies heat to the atmosphere at higher latitudes.

*Richard Wood, Met Office Hadley Centre, and Craig Wallace, National Oceanography Centre*

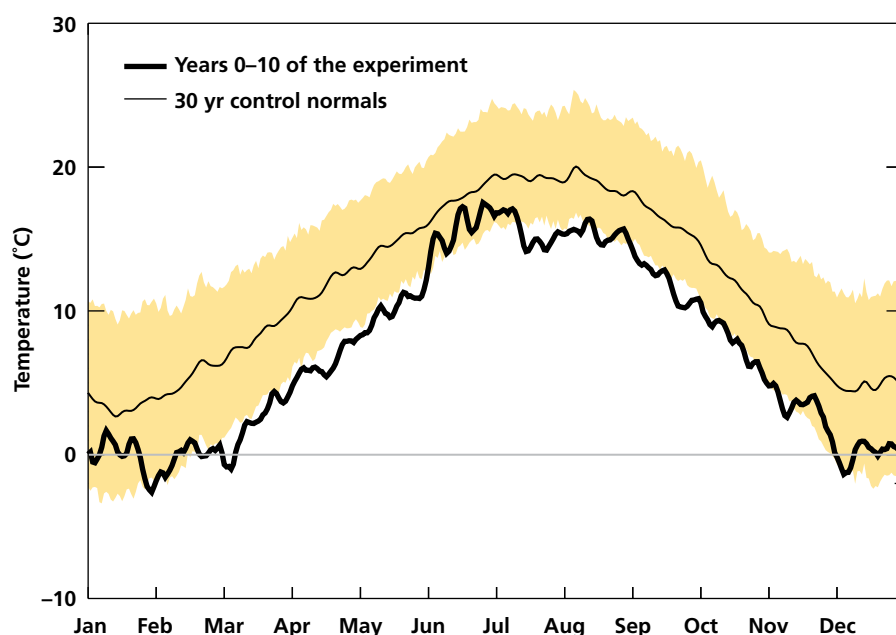


**Figure A5.1:** Daily maximum Central England Temperature from an experiment using the HadCM3 model in which the MOC is artificially switched off (thick curve). Average values over the 10 yr immediately following the switchoff are shown. This is compared with the same quantity in a control run (thin line), with the 5th and 95th percentiles shown by shading. Greenhouse gases are fixed at pre-industrial values in both model runs. Note that the temperatures are derived directly from the global model without downscaling. From Vellinga and Wood (2002).

The effects of the MOC on climate can be estimated using model simulations in which the MOC is artificially switched off by adding fresh water to the North Atlantic. Figure A5.1 shows the modelled impact of a THC shutdown on daily maximum Central England Temperature, relative to the preindustrial climate. A cooling of around 4°C is seen on average, somewhat more in winter than in summer. In spring and autumn this means that the average daily maximum is less than the coldest 5% of days in the pre-industrial climate.

The model also suggests that without the MOC precipitation would be reduced (by around 20% in both summer and winter, averaged over Western Europe as a whole), but that in winter over high ground more precipitation could fall as snow. The MOC also affects regional sea level by redistributing water within the global ocean (without any change in the global average sea level); without the MOC sea level could be around 25 cm higher over some parts of the UK coastline.

Climate models suggest that the MOC will weaken gradually in response to increasing greenhouse gases (see section below). The effects of such a weakening are included in the UKCP09 projections. However concerns have been raised that the MOC might undergo a more rapid decline, or pass a threshold beyond which it will eventually shut down effectively irreversibly. These concerns are based on a range of modelling and theoretical results and on palaeoclimatic evidence. A number of climate models have an MOC that can exist in both a strong, positive state (as today), and in a weak or reversed state. In many of these, if large scale patterns of precipitation and evaporation strengthen beyond a certain threshold, only the weak/reversed state can exist. A number of abrupt changes to the climate of the North Atlantic and adjacent regions in the past have been linked to fluctuations in the strength of the MOC, believed to have been driven by changes in regional fresh water input. Two marked episodes of rapid change, the *8.2 kyr Event* and the *Younger-Dryas Event*, occurring approximately 8200 and 13,000 yr ago respectively, are particularly apparent in recovered ice and sediment core records (e.g. Taylor *et al.* 1997; Thomas *et al.* 2007). Regional temperatures over Greenland are known to have fallen, by ~6°C during the 8.2 kyr Event and by as much as ~15°C during the Younger Dryas Event. Recent work (e.g. Ellison *et al.* 2006) continues to support the hypothesis that the 8.2 kyr Event was driven by the abrupt discharge of fresh glacial melt water from two dammed lakes over continental North America, Agassiz and Ojibwa. In both these past cases, there was more fresh water locked up in land ice than at present, so these periods may not be exact analogues of the present day, but the palaeoclimatic evidence does point to the sensitivity of the MOC to fresh water input.

Since UKCIP02, progress has been made in both observations and modelling of MOC changes.

## A5.2 Is the Atlantic Meridional Overturning Circulation changing?

A number of recent observational studies have attempted to detect signs of recent changes in the MOC. One assessment (Bryden *et al.* 2005) suggests that the overall MOC strength may have decreased by approximately 30% since 1957 (Figure A5.2). However, the sparse nature of the observations used in this study (5 measurements over 5 decades), the possible errors of these observations and the large day-to-day variability of the MOC recently discovered (Cunningham *et al.* 2007; Kanzow *et al.* 2007) highlight the need for additional data to support this conclusion. Furthermore, analyses using Atlantic sea surface temperature patterns as an indirect measurement of MOC strength also conflict with the

conclusion of Bryden *et al.* (2005), citing the recent warming seen in the North Atlantic as indication of a stronger MOC during the 1990s (e.g. Latif *et al.* 2006; Knight *et al.* 2005), although this indirect observational method is based on links identified in climate models rather than directly from observations.

Additional observations farther north also provide evidence for widespread change or variability. For example whilst some studies indicate that, in recent decades, the transport of deep water, forming the return leg of the MOC, through the Faroe Bank Channel (and farther downstream e.g. Bossenkool *et al.* 2007) has decreased by approximately 20% compared to 1950 estimates (Hansen *et al.* 2001), more recent observations (Østerhus *et al.* 2008) call such a trend in to question. Recent large scale freshening of the high latitude North Atlantic, including deep water flowing through the Faroe Bank Channel, has also been the subject of much research (e.g. Dickson *et al.* 2002) but neither the mechanisms of the freshening, nor a clear link with MOC changes, have been established.

In addition to the Faroe Bank Channel, deep returning water also flows through the Denmark Strait, between Greenland and Iceland. Observations within (Macrander *et al.* 2005) and just south (Dickson *et al.* 2008) of the strait do reveal a weakening of the through flow between 1999 and 2003, but this is likely a feature of the natural year-to-year variability, rather than part of any longer-term trend. Deep water from both the Faroe Bank Channel and the Denmark Strait combines south of Greenland to form the Deep Western Boundary Current which is the primary return leg of the MOC south of ~55°N. Measurements of this unified current are also sparse, although comparison of what data is presently available (representing 1993–1995 and 1999–2001, respectively) reveals little change in transport (Schott, 2004).

Knowledge of whether or not the strength of the MOC is changing with time has been hampered to date by the lack of continuous, robust measurements. Since the last UKCIP02 report, however, considerable effort has been made to collate

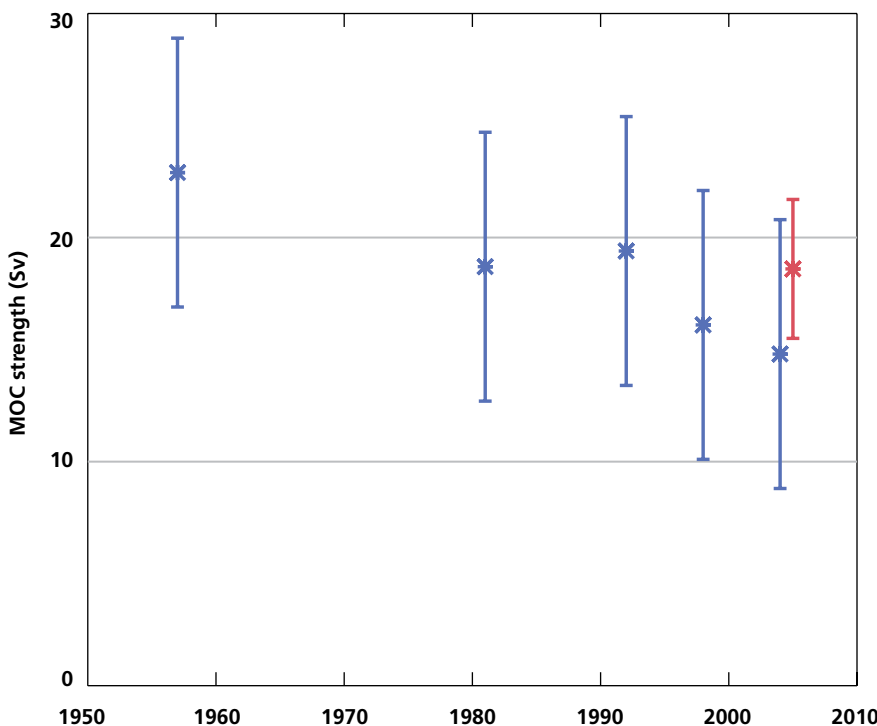


Figure A5.2: Estimates of observed Atlantic MOC strength (asterisks), and associated errors (bars), at ~26°N between 1957 and 2005. Blue denotes calculations incorporating ship-based observations of the free ocean (Bryden *et al.* 2005) whilst the final, red, point incorporates the first year's (April 2004–April 2005) continuous observations from the RAPID mooring array deployed in 2004. The quantity shown is transport in the top 1000 m of the ocean, with positive values indicating northward flow. Units are Sverdrups (1 Sv = 1 million cubic metres of water transported per second).

and analyse existing observations, for example via the ASOF\* initiative, and a substantial UK-led monitoring programme, RAPID, has commenced, involving the installation of permanent moorings at a number of locations within the Atlantic Ocean (see <http://www.nerc.ac.uk/research/programmes/rapid/>). Initial results (Cunningham *et al.* 2007; Kanzow *et al.* 2007) have confirmed the ability of this system of moorings to monitor the MOC to a high degree of accuracy. As the time series accrues to a statistically meaningful length scientists will be able to comment with more certainty on whether any long term change is underway.

### A5.3 Projections of future changes in the Atlantic circulation

Recent projections, using a new generation of climate models, support the assessment presented in UKCIP02 and suggest that the MOC will weaken gradually in response to increasing greenhouse gases. The models examined in the IPCC AR4, excluding those with a poor simulation of the present day MOC, suggest reductions of between 0 and 50% in the MOC by 2100, under the SRES A1B (UKCP09 Medium) emissions scenario. An ensemble of HadCM3-based coupled models, similar to the one used to generate the UKCP09 probabilistic projections, shows a slightly narrower range of weakening under an idealised scenario of CO<sub>2</sub> increase (Figure A5.3). The effects of the gradually weakening MOC on UK climate are included in the UKCP09 climate projections.

No comprehensive climate model, when forced with one of the SRES emissions scenarios, produces a complete or abrupt MOC shutdown in the 21st century,

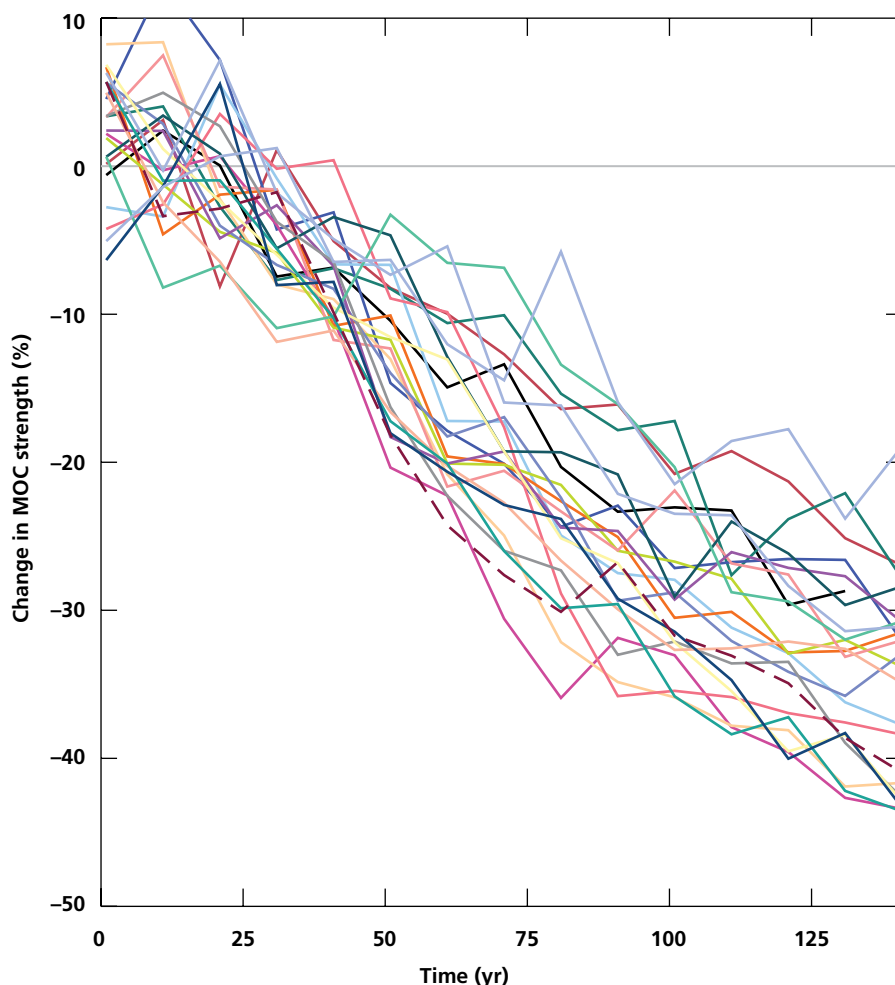


Figure A5.3: Model simulations of the change in MOC strength under an idealised 1%-per-annum increase of CO<sub>2</sub> concentrations. Twenty-two simulations are shown, from a HadCM3-based perturbed physics ensemble similar to the one used to generate the UKCP09 projections. MOC change is expressed as a percentage of its value in the corresponding control run. (Courtesy M. Vellinga.)

\* Arctic-Subarctic Ocean Fluxes <http://asof.npolar.no>

consistent with the models shown in Figure A5.3. However models in general do not allow for the possibility of increased fresh water supply due to rapid ice flow from the Greenland ice sheet, which has been observed in recent years; such extra fresh water could result in further MOC weakening. The simulations of rapid MOC changes that have been seen generally come from less complex climate models; such models are computationally cheaper and so the range of possible behaviours can be explored more fully than with the comprehensive climate models used in UKCP09, but, being simpler, the models may omit key processes affecting the stability of the MOC.

Assessing the evidence overall, the IPCC AR4 concludes that it is very likely (>90% chance) that the MOC will weaken gradually over the 21st century in response to increasing greenhouse gases, but very unlikely (<10% chance) that an abrupt MOC change will occur in that time. Longer term changes cannot be assessed with confidence at this stage.

The effects of any rapid MOC changes (beyond the expected gradual weakening seen in most climate model simulations) would be superimposed on any man-made global climate change that had already taken place. Some of the MOC effects, for example any cooling over the UK, would oppose those due to man. Others, however, would reinforce the global man-made signal — for example additional summer drying, and sea level rise reinforcing that due to thermal expansion.

The figures derived from hypothetical MOC shutdown experiments such as those discussed above show that an MOC shutdown, while very unlikely, could produce climatic effects as large as, or larger than, the effects of increasing greenhouse gases. Thus research to improve our understanding of the probability of such events, and to improve the prospects for early warning, continues to be a priority. Recent developments in both models and observations have improved our fundamental understanding of what controls the MOC, and in time this can be expected to narrow the uncertainty over the future of the MOC.

## A5.4 References

- Boessenkool, K. P., Hall, I. R., Elderfield, H., & Yashayaev, I. (2007). North Atlantic climate and deep-ocean flow speed changes during the last 230 yr. *Geophysical Research Letters*, **34** (doi:10.1029/2007GL030285).
- Bryden, H. L., Longworth, H. R. & Cunningham, S. A. (2005). Slowing of the Atlantic meridional overturning circulation at 25 degrees N. *Nature*, **438**, 655–657.
- Cunningham, S. A., Kanzow, T., Rayner, D., Baringer, M. O., Johns, W. E., Marotzke, J., Longworth, H. R., Grant, E. M., Hirschi, J. J. M., Beal, L. M., Meinen, C. S. & Bryden, H. L. (2007). Temporal variability of the Atlantic meridional overturning circulation at 26.5 degrees N. *Science*, **317**, 935–938.
- Dickson, B., Yashayaev, I., Meincke, J., Turrell, B., Dye, S. & Holfort, J. (2002). Rapid freshening of the deep North Atlantic Ocean over the past four decades. *Nature*, **416**, 832–836.
- Dickson, B., Dye, S., Jonsson, S., Kohl, A., Macrander, A., Marnela, M., Meincke, J., Olsen, S., Rudels, B., Valdimarsson, H. & Voet, G. (2008). The overflow flux west of Iceland: Variability, origins and forcing. In *Arctic-Subarctic Ocean Fluxes*. Dickson, R. R., Meincke, J. & Rhines, P. (Eds). Springer, 736pp.
- Ellison, C. R., Chapman, M. R. and Hall, I. H. (2006). Surface and deep ocean interactions during the cold climate event 8200 yr ago. *Science*, **312**, 1929–1932.
- Hansen, B., Turrell, W. R. & Østerhus, S. (2001). Decreasing overflow from the Nordic seas into the Atlantic Ocean through the Faroe Bank channel since 1950. *Nature*, **411**, 927–930.
- Kanzow, T., Cunningham, S. A., Rayner, D., Hirschi, J. J. M., Johns, W. E., Baringer, M. O., Bryden, H. L., Beal, L. M., Meinen, C. S. & Marotzke, J. (2007). Observed flow compensation associated with the MOC at 26.5 degrees N in the Atlantic. *Science*, **317**, 938–941.
- Knight, J. R., Allan, R. J., Folland, C. K., Vellinga, M. & Mann, M. E. (2005). A signature of persistent natural thermohaline circulation cycles in observed climate. *Geophysical Research Letters*, **32**, L20708.
- Latif, M., Böning, C., Willebrand, J., Biastoch, A., Dengg, J., Keenlyside, N., Schweckendiek, U. & Madec, G. (2006). Is the thermohaline circulation changing? *Journal of Climate*, **19**, 4631–4337.
- Macrander, A., Send, U., Valdimarsson, H., Jonsson, S. & Käse, R. H. (2005). Interannual changes in the overflow from the Nordic Seas into the Atlantic Ocean through Denmark Strait. *Geophysical Research Letters*, **32**, L06606.
- Østerhus, S., Sherwin, T., Quadfasel, D. & Hansen, B. (2008). The overflow transport east of Iceland. In *Arctic-Subarctic Ocean Fluxes*. Dickson, R. R., Meincke, J. & Rhines, P. (Eds). Springer, 736 pp.
- Schott, F.A., Zantopp, R., Stramma, L., Dengler, M., Fischer, J. & Wibaux, M. (2004). Circulation and deep-water export at the western exit of the subpolar North Atlantic. *Journal of Physical Oceanography*, **34**, 817–843.
- Taylor, K. C., Mayewski, P. A., Alley, R. B. *et al.* (1997). The Holocene-Younger Dryas Transition recorded at Summit, Greenland. *Science*, **31**, 278, 825–827.
- Thomas, E. R, Wolff, E. W., Mulvaney, R. *et al.* (2007). The 8.2 Kyr event from Greenland ice cores. *Quaternary Science Review*, **26**, 70–81.
- Vellinga, M. & Wood, R. A. (2002). Global climate impacts of a collapse of the Atlantic thermohaline circulation. *Climatic Change*, **54**, 251–267.

# Annex 6: Future changes in storms and anticyclones affecting the UK

## A6.1 Introduction

*Simon Brown, Met Office Hadley Centre*

It has not been possible to produce probabilistic projections of changes in frequency, strength and location of future storms and anticyclones (often called *blocking* events) — collectively known as synoptic-scale (that is, weather system) variability. This is due to the reasons discussed in Chapter 3, Section 3.3, namely that large differences are found between projections from the Met Office perturbed physics ensemble and those from a multi-model ensemble of alternative climate models (see Figure A6.2). This implies that attempts to construct probabilistic projections would be too dominated by the contribution arising from structural model errors (see Section 3.2.8) to be considered robust. Furthermore, the required storm tracking statistics from other models are not available in any case, thus precluding the use of the UKCP09 methodology (described in Chapter 3) to produce PDFs for this metric. However, storms and blocking events are explicitly modelled in climate models, and the impacts of such synoptic-scale variability and potential changes are considered in the production of PDFs of mean and extreme climate shown elsewhere in this report. Each of the models used in the ensembles which underlie the PDFs, both the perturbed physics and the multi-model, simulate storms and blocking and their integrated impact on those mean and extreme conditions. In addition, the PDFs are constrained by the large-scale observed fields of climate which are partly determined by synoptic-scale variability. In short, the effects of synoptic-scale variability, including potential changes, are taken into account.

Useful information can be gleaned from examination of the present day and future synoptic-scale variability simulated by the Met Office ensemble of 17 HadCM3 experiments (described in Chapter 3, Section 3.2.4) and a multi-model ensemble consisting of 20 alternative coupled models, all using the same SRES A1B (UKCP09 Medium) emissions. Preliminary analysis of these ensembles suggests that the simulated future changes in storms, and their impact on mean climate conditions, are rather modest. Subtle shifts in the position of the North Atlantic storm track are possible, but are inconsistent between different models and different model variants. The frequency and strength of storms remain relatively unchanged in the future simulations, as does the frequency and strength of blocking events. It must be borne in mind, however, that these two ensembles sample a smaller range of uncertainty than do the UKCP09 projections. The IPCC AR4 assessment concluded that the majority of current climate models show a poleward shift of the storm tracks, with some indication of fewer, but deeper, depressions. This can only be concluded when looking at the hemispheric scale;